Recovering IP information in airborne-time domain electromagnetic data

Seogi Kang
University of British Columbia
Vancouver, BC V6T 1Z4 Canada
skang@eos.ub.ca

Douglas W. Oldenburg
University of British Columbia
Vancouver, BC V6T 1Z4 Canada
doug@eos.ubc.ca

SUMMARY

We propose a methodology to generate a 3D distribution of pseudo-chargeability from airborne time domain electromagnetic data. The processing flow is as follows: (a) Apply 3D inversion to TEM data to restore a background conductivity. This might involve omitting responses that are obviously contaminated with IP signals, such as negative transients in coincident loop surveys. The recovered background conductivity is assumed to be uncontaminated by IP signals. (b) Compute the TEM response from the background conductivity and subtract it from the observations. This yields the d^{IP} data, and reduces the EM coupling. (c) The background conductivity is likely not exactly the earth conductivity, but we assume that the major effects of this inaccuracy will lead to a large scale, smoothly varying perturbation to the d^{IP} data. If this correct, then these can be recognized and removed. (d) The final data are linearly related to a pseudo-chargeability through a sensitivity function that is analogous to that employed in usual DC-IP ground surveys. (e) The d^{IP} data at various time channels can be inverted individually. The pseudo-chargeability models may be useful in themselves or they may be further processed to estimate Cole-Cole, or equivalent, parameters. We demonstrate our procedure on a field data set from Mt. Milligan. In the field example, we identify chargeable targets that show no indication of negative transients in the raw data. From the images we can make inferences about the relative strength and geometries of the chargeable bodies.

INTRODUCTION

The electrical conductivity of earth materials can be frequency dependent with the effective conductivity decreasing with decreasing frequency due to the buildup of electric charges that occur under the application of an electric field. Effectively, the rock is electrically polarized. Finding this induced polarization (IP) response has been important in mineral exploration but it is also important in environmental problems, groundwater flow, and site characterization. Polarization charges can accumulate whenever there is an electric field in a medium and so the transmitter can be a galvanic or inductive source. In this study, we focus upon the potential for extracting IP information from airborne systems such as the coincident loop (VTEM) instrument of Geotech Ltd., which measures db_z/dt data. These data are often observed to have negative transients for late time channels. Weidelt (1982) showed that the most plausible explanation of these is that they are caused by IP effects.

Our goal in this paper is to process and invert airborne time domain EM (ATEM) to recover information about the causative chargeable bodies. We use ideas that have been fruitful in the analysis of ground EIP where the IP phenomenon provides a perturbation to the electrical conductivity (Seigel 1959). This allows us to set up a linear inverse problem to recover a pseudo-chargeability. For the technique to work we need to remove any inductive contribution to the signal (that is commonly referred to as EM coupling removal). This requires knowledge of the electrical conductivity, without chargeability effects. We extract that by carrying out a 3D inversion of the airborne data using early time data. A poor estimate for this conductivity can impact upon the quality of the final IP data and we show how those effects can be ameleorated. We apply our technique to field data from Mt. Milligan and verify our approach using synthetic data.

DECOMPOSITION OF IP RESPONSES

A commonly-used expression of complex conductivity model in the frequency domain is the Cole-Cole model (Cole and Cole, 1941):

$$\sigma(\omega) = \sigma_\infty - \sigma_\infty \frac{\eta}{1 + (1-\eta)(\omega\tau)^c},$$

(1)

where σ_∞ is the conductivity at infinite frequency, η is the intrinsic chageability, τ is the time constant and c is the frequency dependency. By applying the inverse Fourier transform we have

$$\sigma(t) = \mathscr{F}^{-1}[\sigma(\omega)] = \sigma_\infty \delta(t) + \triangle\sigma(t)$$

(2)

where $\delta(t)$ is the Dirac delta function and $\mathscr{F}^{-1}[\cdot]$ is the inverse Fourier transform operator. Consider Maxwell's equations in time domain:

$$\vec{\nabla} \times \frac{1}{\mu}\vec{b} - \vec{j} = \vec{j}_s,$$

(3)

$$\vec{\nabla} \times \vec{e} = -\frac{\partial\vec{b}}{\partial t},$$

(4)

where $\vec{e}$ is the electric field (V/m), $\vec{b}$ is the magnetic flux density (Wb/m^2) and μ is the magnetic permeability (H/m). Here $\vec{j}$ is the conduction current. In the frequency domain the current density $\vec{J}$ is related to conductivity via

$\vec{J}(\omega) = \sigma(\omega)\vec{E}(\omega)$. Converting this relationship to time domain using the Fourier transform yields:

$$\vec{j}(t) = \sigma(t) \otimes \vec{e}(t), \tag{5}$$

where $\otimes$ stands for the convolution. That is, the current density depends upon the previous history of the electric field. As in Smith et al. (1988), we let $\vec{e} = \vec{e}^F + \vec{e}^{IP}$, $\vec{b} = \vec{b}^F + \vec{b}^{IP}$ and $\vec{j} = \vec{j}^F + \vec{j}^{IP}$. Here superscripts *F* and *IP* respectively indicate EM responses without IP effects and those only related to polarization. With this decomposition, we write the fundamental and IP current densities as

$$\vec{j}^F(t) = \sigma_\infty \vec{e}^F(t), \tag{6}$$

$$\vec{j}^{IP} = \sigma_\infty \vec{e}^{IP}(t) + \triangle\sigma(t) \otimes \vec{e}(t). \tag{7}$$

Correspondingly, we decompose any type of electromagnetic response, *d*, into fundamental and IP parts so that we have $d = d^F + d^{IP}$. By letting $F[\cdot]$ represent an operator associated with Maxwell's equations, we define the IP datum as

$$d^{IP} = d - d^F = F[\sigma_\infty\delta(t) + \triangle\sigma(t)] - F[\sigma_\infty\delta(t)] \tag{8}$$

This subtraction process acts as an EM decoupling process, which reduces EM effects to better recognize IP effects in the measured responses. This formed the basis of work by Routh and Oldenburg (2001). Thus, assuming that we have a reasonable estimate for the distribution of σ_∞ in 3D space, we can identify the IP signal which is embedded in the measured responses.

3D ATEM-IP INVERSION METHODOLOGY

There are two aspects for time domain inductive source IP that add complexity compared to regular EIP surveys. The first is the convolution term which relates the charge build up to the time history of the electric field. The second is that a steady state charging of the subsurface is never achieved. Rather, at any point in the earth, the electric field will increase and then decay as the inducing fields from the source pass through. The IP signal of interest is usually at those times in which the fundamental field has decayed. Rather than trying to solve the inverse problem to recover the 4D distribution of time dependent conductivity or distributed Cole-Cole parameters we choose a linearization approach that is similar to previous work done for EIP problems

Our linearization is as follows: (a) The most important component of our linearization is IP current density, $\vec{j}^{IP}$. We first formulate a linear relationship between $\vec{j}^{IP}$ and pseudo-chargeability. (b) Once we have $\vec{j}^{IP}$, then $\vec{b}^{IP}$ or $\frac{\partial\vec{b}^{IP}}{\partial t}$ can be computed using Biot-Savart law. Recalling that measured data for inductive sources are $\vec{b}$ or $\frac{\partial\vec{b}}{\partial t}$, TEM responses can be linearized as a function of pseudo-chargeability. In order to linearize $\vec{j}^{IP}$, we first rewrite total electric field as

$$\vec{e}(t) = \vec{e}^F_{max}w^e(t) \tag{9}$$

where $\vec{e}^F_{max} = \vec{e}^F(t) \otimes \delta(t - t^{max})$, is the maximum fundamental electric field and $w^e(t)$ is a dimensionless function that prescribes the history of the electric field at each location. $\vec{e}^F_{max}$ is an appropriate scaling for the electric field since the maximum IP response that could be expected is

when $\vec{e}^F_{max}$ would have constantly applied. Combining equations (7) and (9), yields

$$\vec{j}^{IP}(t) = \sigma_\infty \vec{e}^{IP}(t) + \triangle\sigma(t) \otimes w(t)\vec{e}^F_{max}$$
$$= \sigma_\infty \vec{e}^{IP}(t) - \sigma_\infty \tilde{\eta}(t)\vec{e}^F_{max} \tag{10}$$

where pseudo-chargeablity:

$$\tilde{\eta}(t) = -\frac{\triangle\sigma(t) \otimes w^e(t)}{\sigma_\infty} \tag{11}$$

To compute $\vec{e}^{IP}$ in equation (10), we assume $\frac{\partial\vec{b}^{IP}}{\partial t} \approx 0$, so that we $\vec{e}^{IP}$ can be expressed as

$$\vec{e}^{IP} \approx -\vec{\nabla}\phi^{IP} \tag{12}$$

With this assumption and the fact that $\nabla \cdot \vec{j}^{IP} = 0$ it can be shown that $\vec{j}^{IP}$ can be approximated as

$$\vec{j}^{IP}(t) \approx \vec{j}^{IP}_{approx} = -\bar{S}\sigma_\infty \vec{e}^F_{max}\tilde{\eta}(t) \tag{13}$$

where $\bar{S} = -\sigma_\infty\vec{\nabla}[\nabla \cdot \sigma_\infty\vec{\nabla}]^{-1}\nabla \cdot +\bar{I}$ and $\bar{I}$ is the identity tensor. This equation is significant, since the only time-dependent term is the pseudo-chargeability. Therefore, the IP current density can be considered as instantaneous property. This allows us to compute, for each time channel, the d^{IP} responses using the Biot-Savart law:

$$\frac{\partial\vec{b}^{IP}}{\partial t}(\vec{r};t) = \frac{\mu_0}{4\pi}\frac{\partial}{\partial t}\int_\Omega \frac{\vec{j}^{IP}(\vec{r}_s;t) \times \hat{r}}{|\vec{r} - \vec{r}_s|^2}dv_s$$
$$\approx -\frac{\mu_0}{4\pi}\frac{\partial}{\partial t}\int_\Omega \frac{\bar{S}\sigma_\infty\vec{e}^F_{max}(\vec{r}_s) \times \hat{r}}{|\vec{r} - \vec{r}_s|^2}\tilde{\eta}(t)dv_s \tag{14}$$

By discretizing this equation, we have a linear equation

$$\mathbf{d}^{IP}(t) = -\mathbf{J}\tilde{\eta}(t), \tag{15}$$

where **J** is the sensitivity matrix, which is dependent on background conductivity. This is a linear relationship between the data and pseudo-chargeability. Following Oldenburg and Li (1994) we formulate the inverse problem and calculate a pseudo-chargeability distribution at each time channel.

Much of the success of the above strategy rests upon the ability to have a good estimate of the background conductivity. This is needed to generate the data and also the sensitivity function in the linear system. We have the capability to efficiently carry out 3D ATEM inversion (Yang 2013). Before carrying out this inversion, data that are obviously contaminated with IP signal, (e.g. time channels with negative values) are first winnowed. Irrespective of how well this is carried out, there may be some residual error left in the data. In synthetic cases where our background conductivity is scaled up or down by a factor, this error manifests itself as a DC shift in the d^{IP} data. If the value of the shift can be estimated from the d^{IP} data then the effect of the incorrect background can be removed. This motivates us to work with the d^{IP} data and estimate a smoothly varying background field, which when subtracted from the d^{IP} data, yields data for inversion. This procedure will work only if the scale of the perturbation from the incorrect background model is larger than the length scale of the IP signal, that is, the two signals must be separable. Our scenario is thus analogous to common works in potential fields where a background gravitational or magnetic field must be removed to reveal the anomalous field to be inverted. Thus, in practice, we can redefine our IP datum as

$$d^{IP} = d^{obs} - d[\sigma_{est}] - \delta d = raw\ d^{IP} - \delta d \tag{14}$$

where σ_{est} is the background conductivity model estimated from 3D ATEM inversion, $d[\sigma_{est}]$ is the forward modelled data from σ_{est}, and δd arises from the regional processing. Here let *raw* $d^{IP} = d^{obs} - d[\sigma_{est}]$.

FIELD EXAMPLE: MT. MILLIGAN

In 2007 a VTEM survey was flown over the Mt. Milligan deposit as part of QUEST project initiated by Geoscience of BC. A location map and soundings along a profile are shown in Figure 1a and b, respectively. Note the strong negative transients near 800 m distance. The data were inverted in 3D (Yang et al., 2014) and the recovered conductivity model is shown in 3D (Figure 1c). The conductivity inversion omitted some stations/time channels where the measured responses showed strong negative transients. By using this 3D conductivity model, we computed d^{IP} data using equation (8).
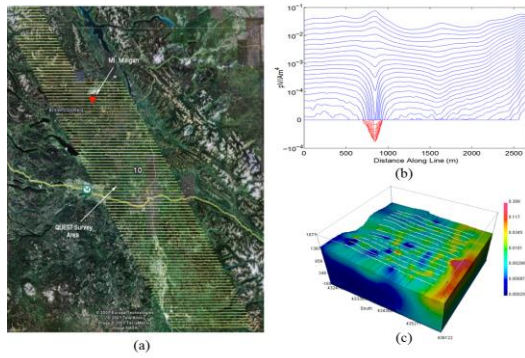

Figure 1: Geographic location of Mt. Millgan (a). Profile of negative transients observed in a VTEM survey at the Mt. Milligan deposit in British Columbia (b). Estimated background conductivity model from 3D ATEM inversion (Yang et al., 2013).

In Figure 2, we present observed data, predicted data from 3D ATEM inversion and d^{IP} data. Here we put white and black dashed circles to emphasize five d^{IP} anomalies; black dashes indicate locations where negative transients are observed in the raw data (A2,A3). White dashes indicate anomalies where transients are noted after EM coupling removal (A1, A4, A5). At 7.2 ms we can clearly observe negative transients near (A2,A3) anomalies, whereas we cannot see negative transients near (A1, A4, A5). However, by subtracting predicted data, we can clearly recognize all five anomalies as shown in right panel of Figure 2.

The next step is to account for inexact knowledge about the background conductivity. For each time channel we estimate a regional by fitting the observed data with a low order polynomial then subtract this regional from d^{IP}. In addition, based on the knowledge that d^{IP} data should be negative at late time channels for a coincident loop system, we replace all positive values in regional-removed d^{IP} data with zeros. The d^{IP} data, the estimated regional, and the corrected data at t = 7.2 ms are shown in Figure 3. These maps convey much information of existence of IP anomalies.

The final step is to carry out the inversion. In Figure 4, we present a 3D pseudo-chargeability model which is estimated from our linear inversion of d^{IP} data t = 7.2 ms. We can recognize that anomalous d^{IP} responses are reasonably mapped in the 3D space and we also observe the changes of anomalous IP bodies in depth.
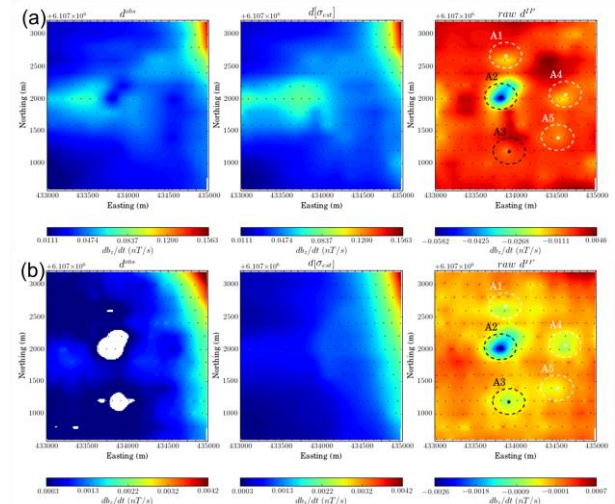
Figure 2: Observed (left panel), predicted (middle panel), d^{IP} (right panel) data from 3D ATEM inversion of Mt. Milligan VTEM data. Responses at (a) t=4.8 and (b) t=7.1 ms. Solid dots indicate sounding locations and dashed circles outline five d^{IP} anomalies (A1-A5). Black and white colors of dashed circles differentiate two different types of d^{IP} anomalies.
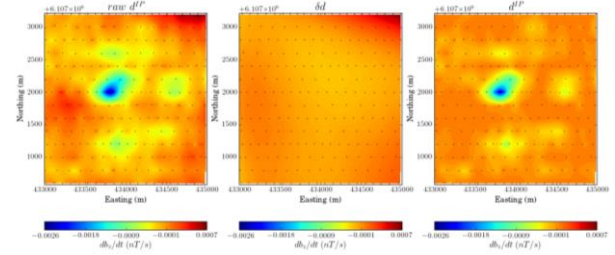
Figure 3: Regional removal process of Mt. Millgian data. (a) *raw* d^{IP} responses (b) estimated regional field, δd (c) d^{IP} responses
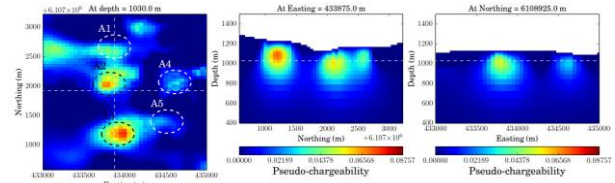
Figure4: Recovered 3D pseudo-chargeability model by inverting field d^{IP} data at t=7.2 ms. Left panel shows plan view, and middle and right ones show vertical section intersecting Northing and Easting lines, respectively.

In order to test the reliability of our inversion procedure and methodology, we perform a synthetic study. We use the EMTDIP code developed by Marchant et al. (2012), which computes forward responses of time domain EM with a Cole-Cole model. Background conductivity model estimated from 3D ATEM inversion is used as σ_{∞} and the synthetic η model is shown in Figure 5; τ for all IP bodies is fixed to 0.008. Based on the field data inversion result, we inserted five isolated bodies, which have different Cole-Cole parameters. Corresponding Cole-Cole parameters for each IP body are given in Figure 5. Generated synthetic data with, and without, consideration of IP effect at t=0.7 and 1.3 ms are shown in left and middle panels of Figure 6, respectively; d^{IP} responses at those time channels are shown on the right panel of Figure 6.

By comparing Figures 2 and 6, we observe similar trends in the observed, predicted and d^{IP} data in both field and synthetic cases. Linearized inversion is applied to the synthetic d^{IP} data at t=1.3 ms, and the recovered 3D pseudo-chargeability distribution is shown in Figure 7. IP bodies near (A2, A3, A4) are reasonably recovered, whereas those near (A1, A5) show blurred distributions. This is due to relatively small d^{IP} anomalies near those regions.
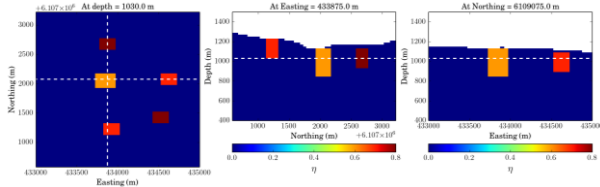

Figure 5: Synthetic 3D chargeability model.

To summarize, five anomalies are identified from Mt. Milligan VTEM field data. Anomalies at A2, A3 exhibited negative values at mid to late times and hence would have been identified as locations of chargeable material. Anomalies at A1, A4, A5 were not associated with negatives and are observed only because of the decoupling process. With the synthetic study based on the field configuration, we show that these time decaying features can be explained by forward modelling TEM responses with a Cole-Cole model. In addition, comparison of recovered pseudo-chargeability models between synthetic and field d^{IP} data provide some confidence in the reliability of our inversion methodology and field data inversion results.
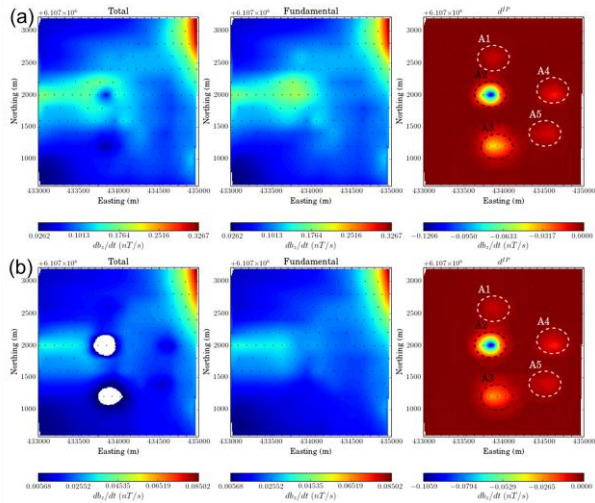

Figure 6: Synthetic total (left panel), fundamental (middle panel), d^{IP} (right panel) responses.   Responses at (a) t=0.7 and (b) t=1.3 ms (b).
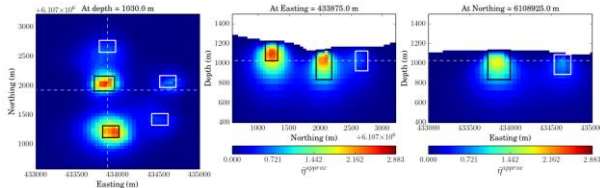

Figure 7: Recovered 3D pseudo-chargeability model from synthetic d^{IP} data at t=1.3 ms.

CONCLUSIONS

In this study we have developed a procedure to recover distributed IP information from ATEM data. The processing contains estimation of a background conductivity, removal of EM coupling, estimation of a possible residual field induced by incorrect conductivity distribution of the earth and carrying out a linearized inversion to recover a pseudo-chargeability. The inversion has been done at each time channel and the results are analysed to extract intrinsic estimates of the Cole-Cole parameters. We identify that there are considerable assumptions that have gone into generating our algorithm, principally the need to estimate the background conductivity and the assumption that we can estimate a residual field that can be removed from the data. These are issues for further research. Nevertheless, the success we have had in applying the technique to the Mt. Milligan data shows the potential for finding IP bodies from time domain airborne data.

REFERENCES

Kang, S., Oldenburg D. W., D. Yang, and D. Marchant, 2014, On recovering induced polarization information from airborne time domain EM data: 84th meeting SEG, Denver, Expanded Abstracts, 1785–1789.

Cole, K. S. and Cole, R. H., 1941, Dispersion and absorption in dielectrics i. alternating current characteristics: The Journal of Chemical Physics, 9(4), 1941.

Marchant, D., Haber, E., Beran, L., and Oldenburg, D. W., 2012, 3D modeling of IP effects on electromagnetic data in the time : 82th meeting SEG, Las Vegas, Expanded Abstracts, 1-5.

Oldenburg, D. W. and Li., Y., 1994, Inversion of induced polarization data: Geophysics, 59(9), 1327–1341.

Routh, P. S. and Oldenburg D. W., 2001, Electromagnetic coupling in frequency-domain induced polarization data: a method for removal: Geophysical Journal International, 145(1):59–76, 2001

Seigel, H., Mathematical formulation and type curves for induced polarization: Geophysics, 24(3):547–565, 1959.

Smith, R., Walker, P., Polzer, B., and West, G. F., 1988, The time-domain electromagnetic response of polarizable bodies: an approximate convolution algorithm: Geophysical Prospecting, 36, 772–785.

Weidelt, P., 1982, Response characteristics of coincident loop transient electromagnetic systems: Geophysics, 47, 1325–1330.

Yang, D., Oldenburg, D. W., and Haber, E., 2014, 3-d inversion of airborne electromagnetic data parallelized and accelerated by local mesh and adaptive soundings: Geophysical Journal International, 196, 1942–1507.